Supplemental Information

Structural dynamics of the functional nonameric Type III translocase export gate

Biao Yuan[1,2,3,4], Athina G. Portaliou[1], Rinky Parakra[1], Jochem H. Smit[1,5], Jiri Wald[2,3,4], Yichen Li[5], Bindu Srinivasu[1], Maria S. Loos[1], Harveer Singh Dhupar[6], Dirk Fahrenkamp[2,3,4], Charalampos G. Kalodimos[7], Franck Duong van Hoa[5], Thorben Cordes[5,8], Spyridoula Karamanou[1], Thomas C. Marlovits[2,3,4,9] and Anastassios Economou[1,9,10]

[1] KU Leuven, Department of Microbiology and Immunology, Rega Institute for Medical Research, Laboratory of Molecular Bacteriology, B-3000 Leuven, Belgium
[2] Centre for Structural Systems Biology (CSSB), Notkestrasse 85, D-22607 Hamburg, Germany
[3] University Medical Center Hamburg-Eppendorf (UKE), Institute for Structural and Systems Biology, Notkestrasse 85, D-22607 Hamburg, Germany
[4] German Electron Synchrotron Centre (DESY), Notkestrasse 85, D-22607 Hamburg, Germany
[5] Molecular Microscopy Research Group, Zernike Institute for Advanced Materials, University of Groningen, Nijenborgh 4, 9747 AG Groningen, The Netherlands
[6] Department of Biochemistry and Molecular Biology, Faculty of Medicine, Life Sciences Institute, University of British Columbia, Vancouver, Canada
[7] Department of Structural Biology, St. Jude Children's Research Hospital, 263 Danny Thomas Place, Memphis, Tennessee 38105
[8] Physical and Synthetic Biology, Faculty of Biology, Ludwig Maximilians-Universität München, Großhadernerstr. 2-4, 82152 Planegg-Martinsried, Germany

[9]For correspondence: Anastassios Economou (tassos.economou@kuleuven.be)
Thomas C. Marlovits (thomas.marlovits@cssb-hamburg.de)
[10] Lead contact

Abbreviations

AHT: Anhydrotetracycline
BN-PAGE: Blue native PAGE
CN-PAGE: Clear native PAGE
DDM: *n*-Dodecyl-β-D-maltopyranoside
EPEC: Enteropathogenic *E. coli*
GPC-MALS/QELS: Gel permeation chromatography coupled to multi-angle light scattering and quasi-elastic light scattering detectors
IMVs: Inverted Membrane Vesicles
IPTG: Isopropyl β-D-1-thiogalactopyranoside
T3S: Type 3 Secretion
T3SS: Type 3 Secretion System
TCA: Trichloroaetic Acid
Triton: Triton X-100

Table of contents

Supplementary Figures

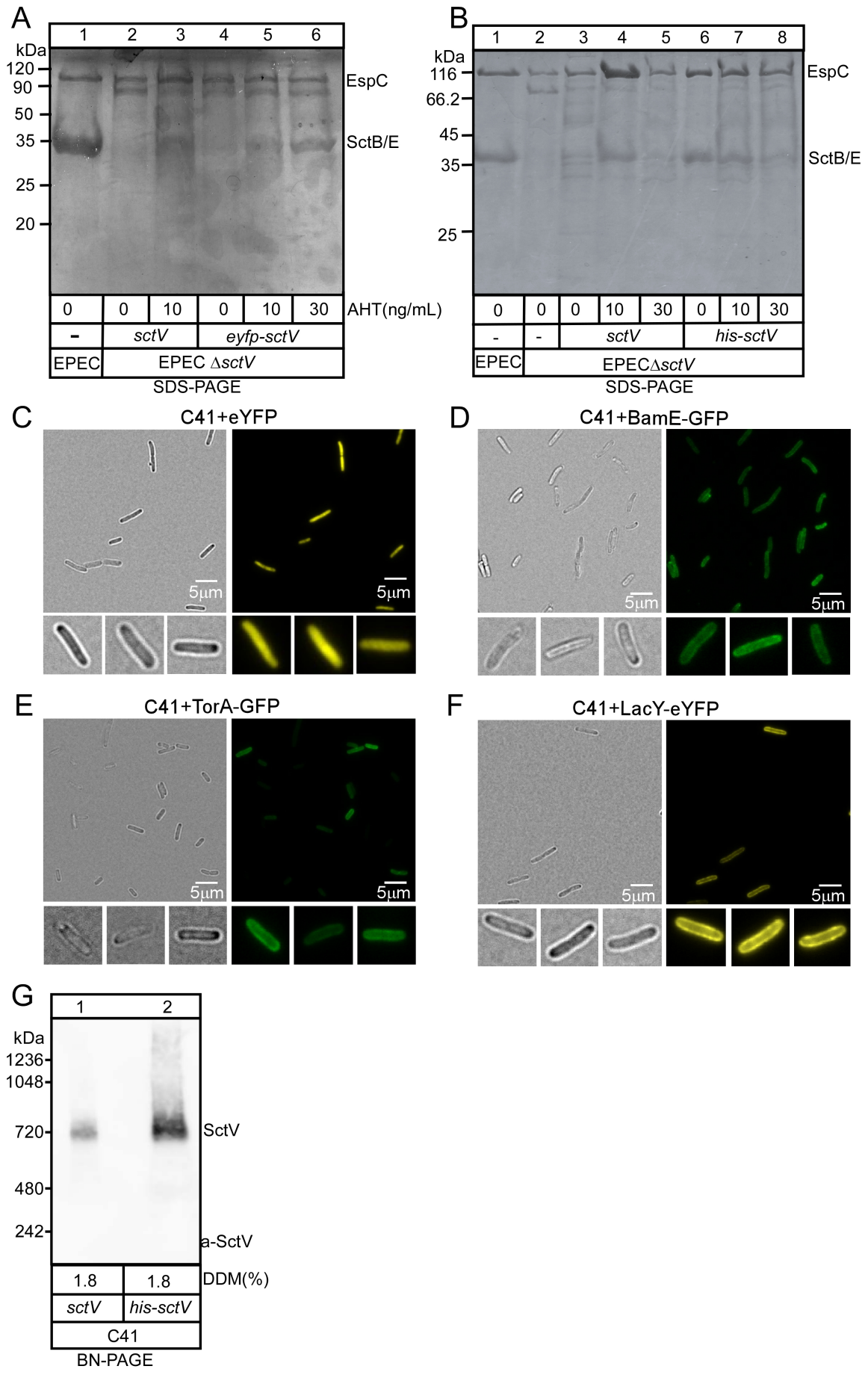

Fig. S1: SctV derivatives can restore Type III secretion in EPEC∆*escV* (related to Figures 1 and 3).

A and B. *In vivo* secretion of EPEC∆*sctV* carrying a plasmid with either *sctV*, or *eyfp-sctV* **(A)** or *his-sctV* **(B).** Gene expression was induced with different AHT concentrations as indicated. Secreted proteins from spent growth medium were TCA-precipitated. Equal volume of spent medium corresponding to equal number of cells were analyzed by SDS-PAGE, followed by coomassie blue staining. The EspC and the translocators SctB/E were indicated. Representative images are shown; *n=3.*

C-F. The distribution of control protein markers in C41 cells. The fluorescence micrographs of C41 cells expressing eYFP (**D**), TorA-GFP (**E**), BamE-GFP (**F**), and LacY-eYFP (**G**) separately. Scale bar: 5μm. Representative images from YFP or GFP (as indicated) and brightfield channel are shown; n=3 biological replicates

G. SctV and His- SctV can form nonameric species. The membrane fractions derived from C41 cells carrying pACYCDuet-*sctV* (lane 1) or *his-sctV* (lane 2) were treated with 1.8% DDM, analyzed by BN-PAGE and immuno-staining with α-SctV-C. Representative images are shown; *n=3.*

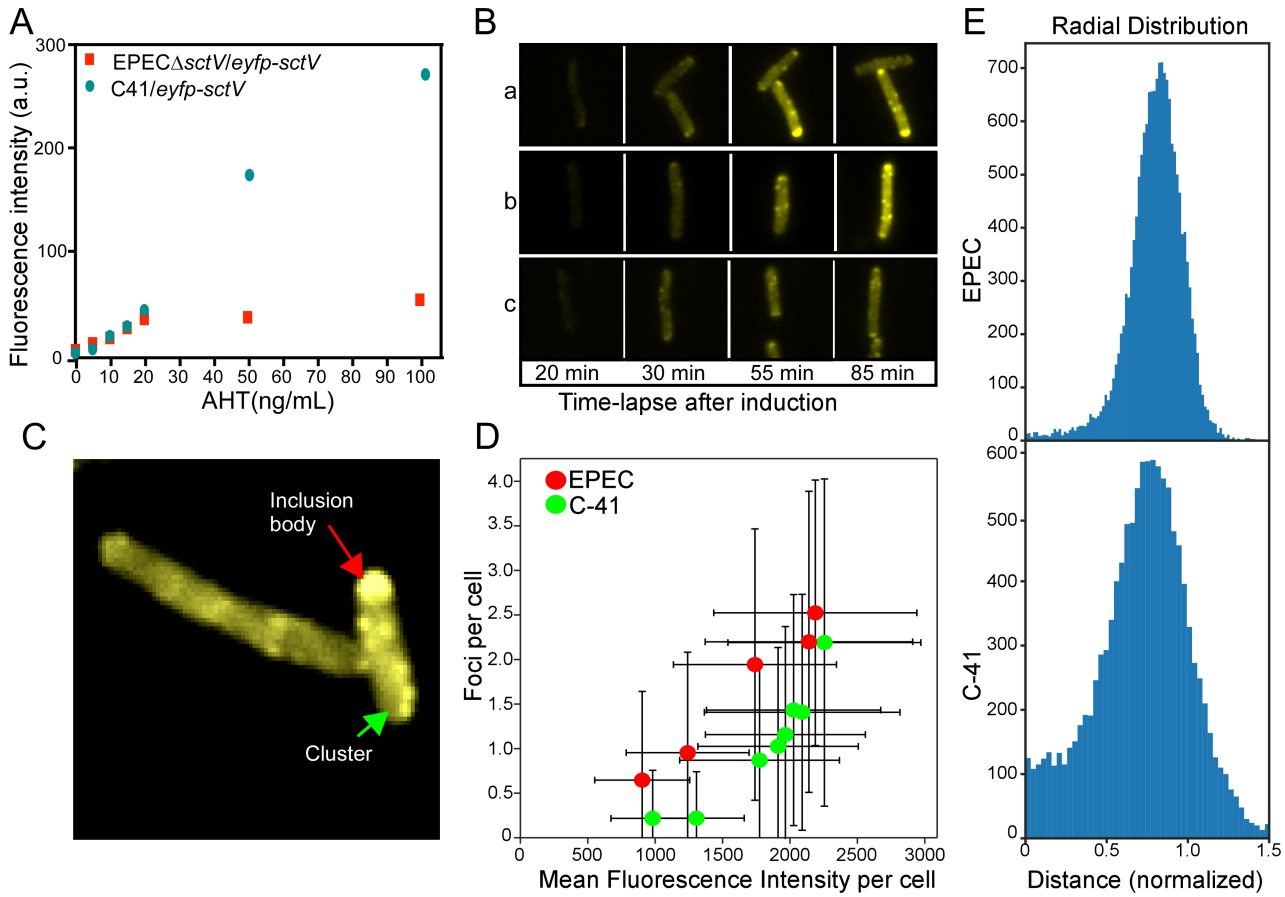

Fig. S2: eYFP-SctV production, foci formation, and distribution in C41 or EPECΔ*sctV* (related to Figure 1).

A. Comparison of the *eyfp-sctV* expression levels in C41 cells (blue) and EPECΔ*sctV* strain (red). Bacterial cells were grown in LB and induced (37°C; OD_{600}: 0.3) with different AHT concentrations for 3 hours. The fluorescence intensity of total cells was measured (Infinite 200 PRO microplate reader; TECAN) and used as an indicator of *eyfp-sctV* expression level. 20 ng/mL AHT was used for further experiments so to achieve similar protein production in both strains. *n=3* biological replicates

B. Foci formation in C41 cells expressing *eyfp-sctV*. Time lapse images were acquired every 5 min for 90 min upon induction of *eyfp-sctV* expression with 20 ngr/ml AHT. Three slices (a, b, c) are shown at different time points as indicated. *n=3* biological replicates

C. Inclusion body formation in C41 cells expressing *eyfp-sctV*. Inclusion body (red arrow) was distinctly larger and polarly located as compared to normal *eyfp-sctV* clusters (green arrow) and was excluded from statistical analysis.

D. Quantification of fluorescent foci in EPEC and C41 cells. Number of detected foci per cell for EPEC and C41 cells expressing *eyfp-sctV* were plotted as a function of the mean fluorescence intensity per cell (arbitrary units). Each data-point represents an individual microscopy experiment, error bars are standard deviations. *n=5-7* biological replicates

E. Foci distribution across cells. Radial distributions of fluorescent foci in EPEC (upper panel, *n=10,770*) and C41 (bottom, *n=14,209*) cells. Radial distances were measured from the center of the cell and normalized with respect to the cell's radius. Cell radius was measured from the brightfield image.

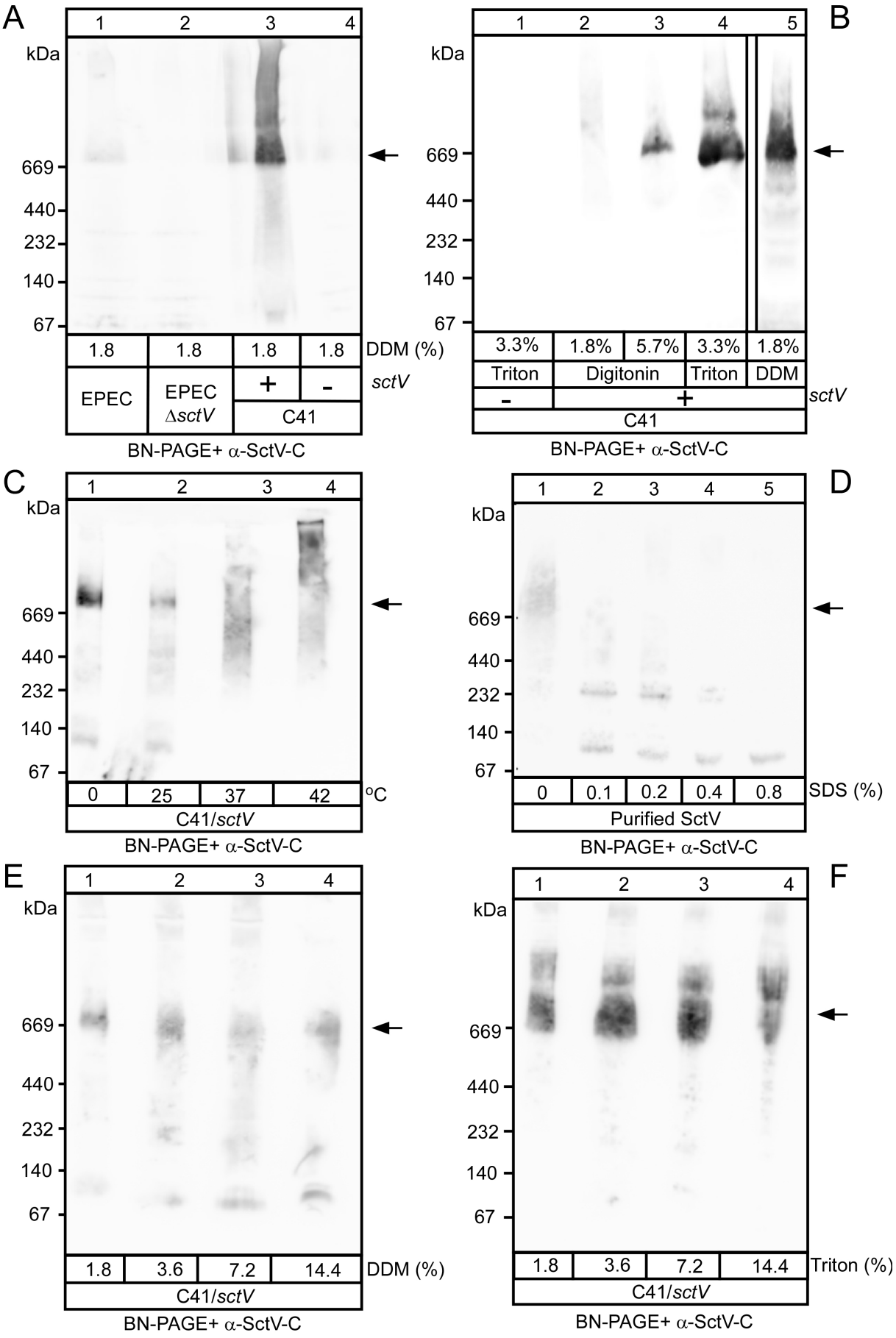

Fig. S3: Stability of the SctV nonameric complex (related to Figures 1 and 3).
A. Comparison of the *sctV* expression in EPEC (lane 1) and C41/pACYCDuet-1-*sctV* (lane 3). Membrane fractions were extracted with 1.8% DDM and samples were analyzed by BN-

PAGE and α-SctV-C immuno-staining. 30 μl of EPEC derived membrane extracts and 5 μl from C41 (40mg/ml) were loaded on gel. Signal intensities were quantified using Image J software. >50-fold more SctV synthesis is observed in C41/pACYCDuet-1-*sctV* compared to that in EPEC; Representative images are shown; *n=3. Arrow:* $SctV_9$.

B. The $SctV_9$ species can be extracted with different non-ionic detergents. Membrane extracts (20 μl loading; 40mg/mL membrane protein) from C41 carrying the pACYCDuet-1-*sctV* were treated with the indicated non-ionic detergents and analyzed by BN-PAGE and α-SctV-C immuno-staining. Representative images are shown; *n=3*.

C. High temperature causes $SctV_9$ aggregation. Membrane fractions were extracted (as in A) with 1.8% Triton X-100 and incubated at different temperatures (as indicated; 30 min). Samples were analyzed by BN-PAGE (20 μl loading; 40mg/mL) and α-SctV-C immuno-staining. Representative images are shown; *n=3.*

D. Ionic detergent (SDS) disassembles $SctV_9$. Purified His-SctV (2 μg; 200 ng/μl) was treated with different amounts of SDS (as indicated; 30 min; 4ºC) and then analyzed by BN-PAGE and α-SctV-C immuno-staining. Representative images are shown; *n=3*.

E and **F.** $SctV_9$ is resistant to high concentration of non-ionic detergents. The membrane fractions of C41/*sctV* were extracted with different high concentrations of DDM (**E**) or Triton X-100 (**F**) and then analyzed by BN-PAGE and α-SctV-C immuno-staining. Representative images are shown; *n=3.*

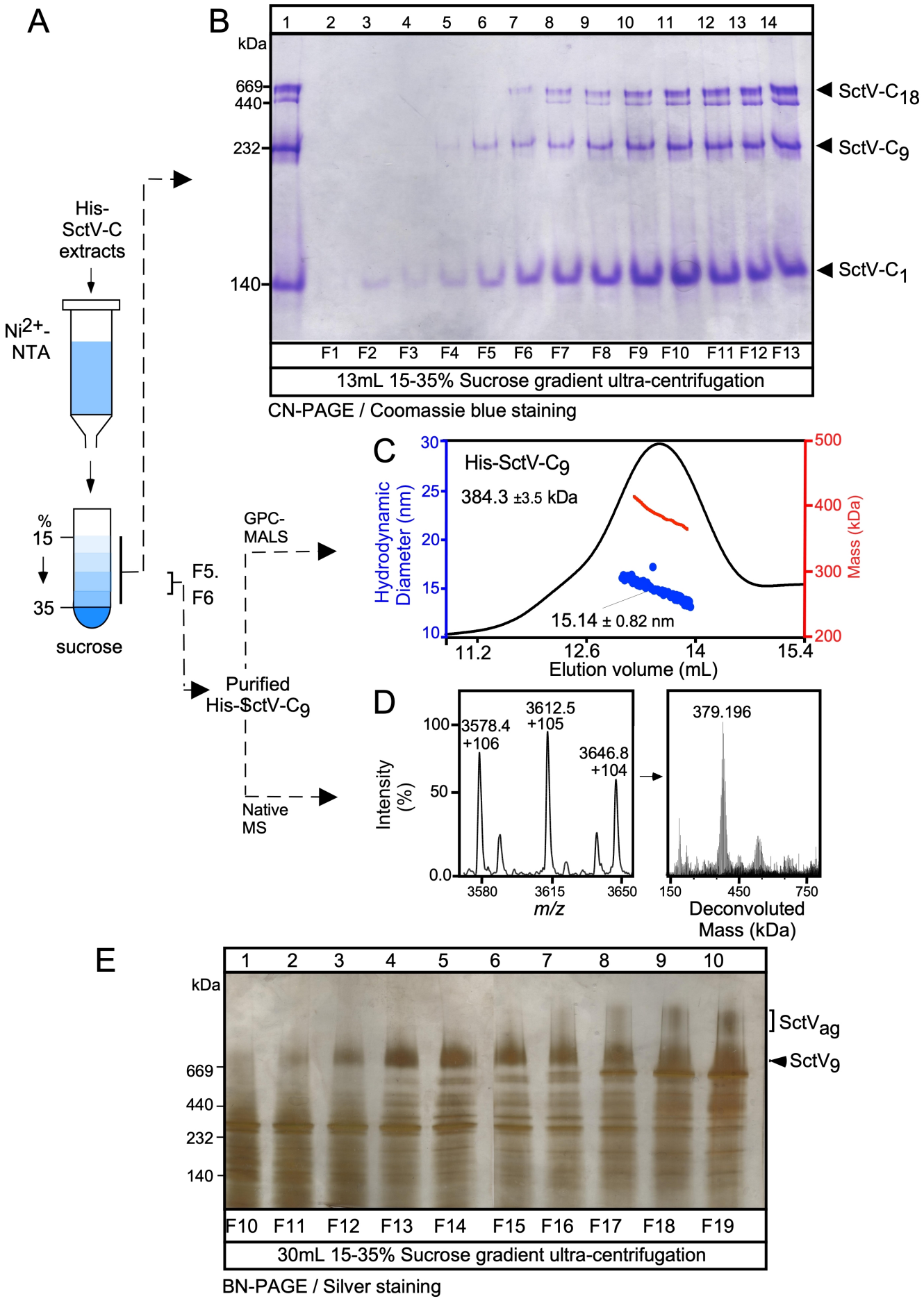
A
His-SctV-C extracts
Ni2+-NTA
%15
35
sucrose
F5.
F6
GPC-MALS
Purified His-SctV-C9
Native MS
B
kDa
669
440
232
140
1 2 3 4 5 6 7 8 9 10 11 12 13 14
F1 F2 F3 F4 F5 F6 F7 F8 F9 F10 F11 F12 F13
13mL 15-35% Sucrose gradient ultra-centrifugation
SctV-C18
SctV-C9
SctV-C1
CN-PAGE / Coomassie blue staining
C
His-SctV-C9
384.3 ±3.5 kDa
15.14 ± 0.82 nm
Hydrodynamic Diameter (nm)
Mass (kDa)
Elution volume (mL)
D
3578.4 +106
3612.5 +105
3646.8 +104
379.196
Intensity (%)
m/z
Deconvoluted Mass (kDa)
E
kDa
669
440
232
140
1 2 3 4 5 6 7 8 9 10
F10 F11 F12 F13 F14 F15 F16 F17 F18 F19
30mL 15-35% Sucrose gradient ultra-centrifugation
SctVag
SctV9
BN-PAGE / Silver staining

Fig. S4: Purification of $SctV_9$ and $SctV\text{-}C_9$ (related to Figures 2, 3 and 4)

A. Purification of the C-terminal cytoplasmic domain His-$SctV\text{-}C_9$ using sucrose gradient (15-35% w/v) centrifugation. 500μl (10 mg/mL) His-SctV-C purified from Ni^{2+}-NTA resin was loaded on top of a pre-formed sucrose gradient and harvested in 13 fractions (1mL each).

B. Fractions F1 to F13 from A, (20μl loaded) were analyzed by CN-PAGE and stained with coomassie blue (see Materials and Methods for details). Fractions with the dimerized 9-meric species were discarded (F6-F13, lanes 7 to 14), while fractions containing nonameric and monomeric species (F5 and F6, lanes 4 and 5) were used for further analysis in C and D. L, loading sample; the $SctV\text{-}C_{18}$, $SctV\text{-}C_9$, and SctV-C are indicated. The monomeric species migrates aberrantly in CN-PAGE near the position of the 140kDa protein marker but is resolved as a clear monomer by gel permeation chromatography coupled on line with MALS as a species of 45kDa (-/+2). Representative images are shown; *n=5*

C. Purified pooled fractions F5/F6 of His-$SctV\text{-}C_9$ from A and B (around 50 μM; Buffer M) were analyzed using GPC with online MALS and QELS measurements. SctV-C migrated as a broad peak with a determined mass of 380.9 ± 3.8 kDa and with a hydrodynamic radius of 15.04 ±0.82 nm that would be close to the theoretically expected values of a 9-mer ($SctV\text{-}C_9$; theoretical mass 365,34 kDa). UV traces (black) and hydrodynamic radius (blue); Mass (red). *n=3*

D. Electrospray Ionization Mass Spectrometry (ESI-MS) analysis of native His-$SctV\text{-}C_9$ purified in B. The spectrum of His-$SctV\text{-}C_9$ at different charge states (left panel) and its deconvolution into a native mass (right panel) are shown. *n=3*

E. Analysis of fractions of full-length His-$SctV_9$ after separation in a sucrose gradient (15-35% w/v) upon ultra-centrifugation. Membrane proteins were extracted (1.8% Triton X-100) from membranes prepared from C41/pACYCDuet-1-*his-sctV* cells after disruption by French press and ultracentrifugation. Detergent-solubilized membrane proteins were separated using a linear sucrose gradient. Sucrose gradient fractions (1mL each; 20μl loaded on the gel) were analyzed by BN-PAGE and stained with silver staining (lanes 1-10; sucrose gradient fractions #10-19). Higher order aggregates of SctV (bracket; $SctV_{ag}$) were observed in the sucrose gradient fractions F16-19 (lanes 7-10). Fractions F10-15 were collected and pooled for subsequent reconstitution into peptidiscs. A representative gel is shown; *n=5.*

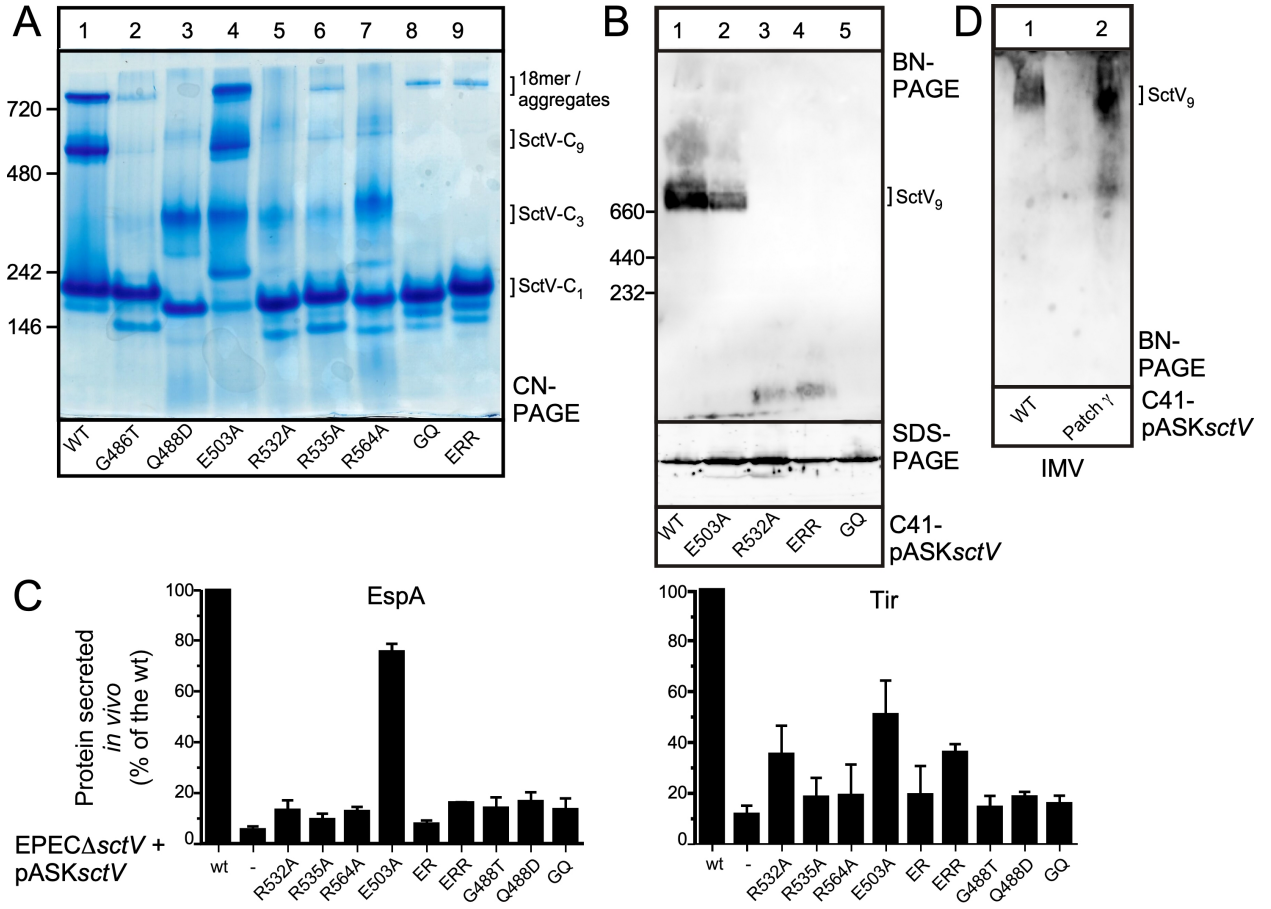

Fig. S5: Analysis of SctV oligomerization mutants (related to Figure 2).

A. CN-PAGE analysis of His-SctV-C wt or mutated at the oligomerization interface (see Fig. S9 below) synthesized in C41 cells. The protein complexes derived from C41/*sctV-C* wt or mutated were purified using Ni-NTA resin and analyzed by CN-PAGE. With the exception of the E503A derivative (lane 4), all other SctV- C derivatives mutated on the oligomerization interface fail to form higher oligomeric species, and display compromised oligomeric complex formation. ERR: E503A-R535A-R564A; GQ: G486T-Q488D. A representative gel is shown; *n=3*

B. BN-PAGE analysis of SctV or of the indicated derivatives mutated in the oligomerization interface synthesized in C41 cells. The membrane fraction of C41 cells expressing plasmid-borne SctV or mutant derivatives was extracted with 1.8% DDM. Samples were analyzed by BN-PAGE (upper panel) and SDS-PAGE (lower panel) and immuno-stained with α-SctV-C antibodies. With the exception of the E503A derivative (lane 2) the other SctV-C mutants fail to form higher oligomeric species, abolishing nonameric complex formation of the full-length protein, despite the fact that all derivatives can be produced intracellularly, like the wild type polypeptide. This indicated that C-domain oligomerization is the driving force for SctV oligomerization. ERR: E503A-R535A-R564A; GQ: G486T-Q488D. A representative gel is shown; *n=6*

C. Secretion of EspA and Tir from EPECΔ*sctV* cells carrying *sctV* or the indicated mutant derivatives. Secreted protein amounts were quantified and secretion derived from EPECΔsctV/ *sctV* was considered 100%. All other values are expressed as % of this. With the exception of the E503A derivative, the rest of the SctV cytoplasmic domain mutants fail to complement protein secretion through T3SS, suggesting that SctV oligomerization is essential for T3SS function corroborating previous observations. ER: E503A-R535A; ERR: E503A-R535A-R564A; GQ: G486T-Q488D. *n=3*.

D. BN-PAGE analysis of SctV or SctV Patch γ-. C41-IMVs carrying SctV or mutant were treated with 1.8% DDM. Samples were analyzed by BN-PAGE and immuno-stained with α-SctV-C antibodies. Mutant SctV can form higher oligomeric species like the wt. A representative gel is shown; *n=5*

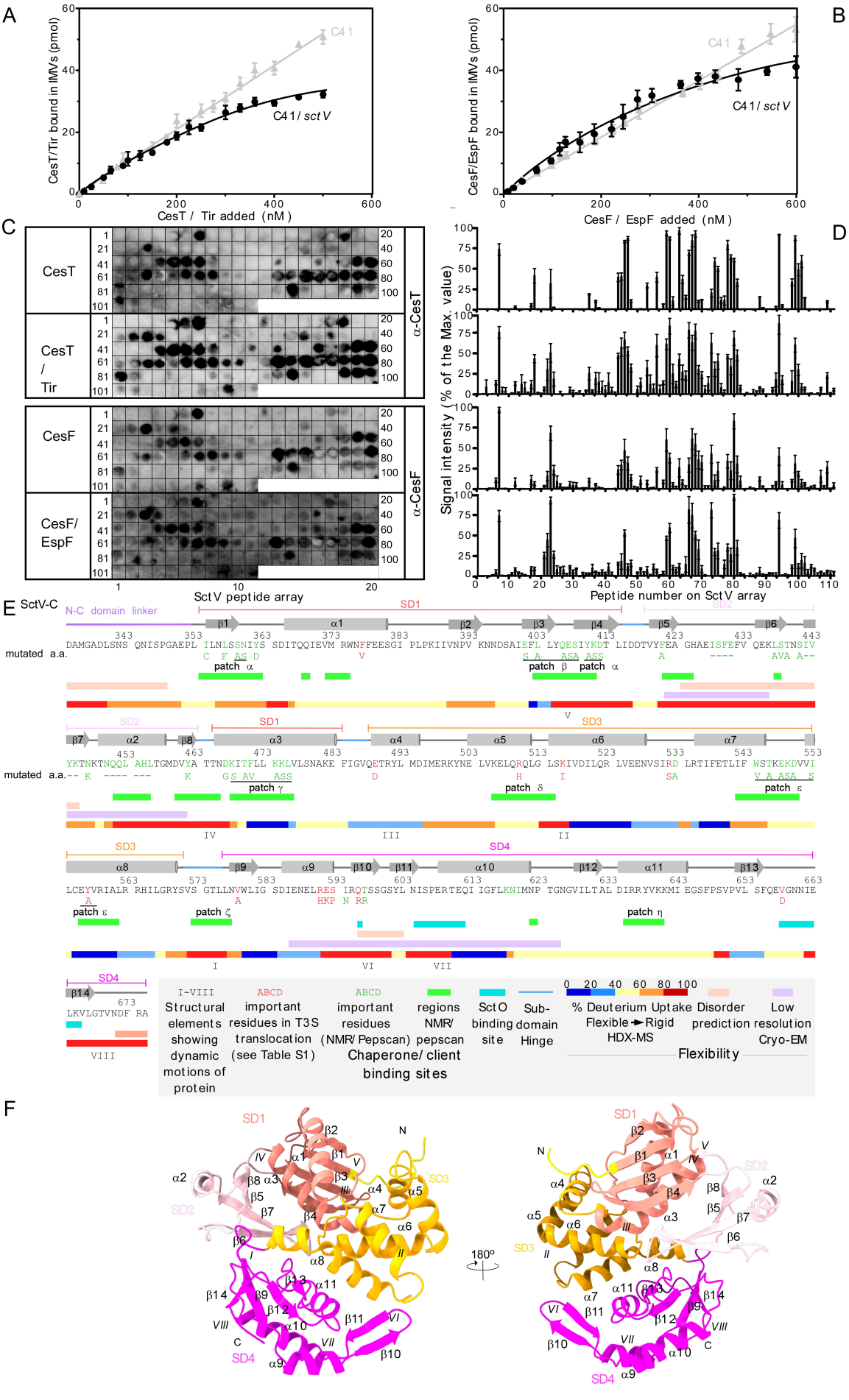
A
CesT/Tir bound in IMVs (pmol)
C41
C41 / sctV
CesT / Tir added (nM)
B
CesF/EspF bound in IMVs (pmol)
C41
C41 / sctV
CesF / EspF added (nM)
C
CesT
CesT / Tir
CesF
CesF/ EspF
α-CesT
α-CesF
SctV peptide array
D
Signal intensity (% of the Max. value)
Peptide number on SctV array
E SctV-C
N-C domain linker
SD1
SD2
SD3
SD4
mutated a.a.
patch α
patch β
patch γ
patch δ
patch ε
patch ζ
patch η
I-VIII Structural elements showing dynamic motions of protein
ABCD important residues in T3S translocation (see Table S1)
ABCD important residues (NMR/ Pepscan) Chaperone/ client binding sites
regions NMR/ pepscan
SctO binding site
Sub-domain Hinge
% Deuterium Uptake Flexible ➔ Rigid HDX-MS
Disorder prediction
Low resolution Cryo-EM
Flexibility
F
180°
N
C

Fig. S6: Binding of chaperone/exported client complexes to full-length, membrane-embedded SctV and to an immobilized array of SctV peptides (related to Figures 2, 5 and 6).

A and **B**. Affinity measurements of chaperone/exported client complexes for membrane-embedded full length His-SctV. The binding curves of [^{35}S]-CesT/Tir and [^{35}S]-CesF/EspF (at concentration ranges of 0-600 nM) for Inner Membrane Vesicles (IMVs) derived from C41 cells with (black) or without (gray) embedded His-SctV$_9$, respectively. Data were analyzed by nonlinear regression in GraphPad Prism 6.0 as described (Portaliou et al., 2017) and represent average values with error bars, standard mean error (SEM) are shown. The interaction of CesT/Tir and CesF/EspF with C41 IMVs exhibited linear, non-saturable binding curves, which did not converge to any K_d. *n = 6-9*.

C-E. Determination of the chaperone/exported client binding sites on SctV-C using an immobilized peptide array.

C. Peptide arrays were used to identify potential chaperone/exported client binding regions on SctV-C. The immobilized peptides (13 mers, with 10 residue overlapping; PepSPOTS™ on Cellulose; JPT) of SctV-C were probed with the indicated purified protein ligands (200 nM; 25 mL Buffer J; 25ºC, 1h): CesT, CesT/Tir, CesF, and CesF/EspF, respectively, as described (Portaliou et al., 2017). Proteins bound to the immobilized peptides were electro-transferred onto PVDF membranes (Amersham GE Life sciences) and immuno-stained with α-CesT and α-CesF antibodies, as indicated. Representative experiments are shown; *n= 6*.

D. The intensity of each peptide obtained from **C** was quantified using ImageQuant software (GE Healthcare). All values per experiment were expressed as a percentage of the highest value and plotted using Graph Pad Prism 6.0; Mean values with error bars (SEM) are shown.

E. Linear map of C-domain of SctV (residues 334-675) including secondary structure elements (numbered only for the presentation and ignoring the unknown elements of the N-terminus). Chaperone binding regions from pepscans (panel C) and from NMR studies of FlhA-C in flagellum (Xing et al., 2018), after sequence alignment with $_{EPEC}$SctV-C, are shown with green lines below the linear sequence of $_{EPEC}$SctV-C. Similarly, SctO binding regions (Jensen et al., 2020), disordered regions (as predicted by IUpred), flexible, intermediate and rigid areas (derived from HDX-MS analysis; coloured as in Fig. 5A) and low resolution cryo-EM regions (Fig. S8) are shown in different colors, as indicated. In addition, structural elements involved in dynamic motions of proteins are shown in latin numerals (I-VIII). The SctV residues mutated in Patch α, β and γ and the chaperone binding regions defined by NMR are indicated in the primary sequence and below them the substituted residues in the mutant derivatives generated [green; (Portaliou et al., 2017; Xing et al., 2018)]. Additionally, after sequence alignment, we indicate important residues for the gatekeeper interaction (red letters) as identified on SctV homologues [see Table S2 for details; (Lee et al., 2014; Shen and Blocker, 2016; Yu et al., 2018)] and below them the substituted residues are indicated.

F: Secondary structural elements and important dynamic motions derived from cryo-EM and HDX-MS analysis respectively are shown in SctV-C protomer. SctV-C sub-domains are colored in a ribbon representation as in Fig. 4E.

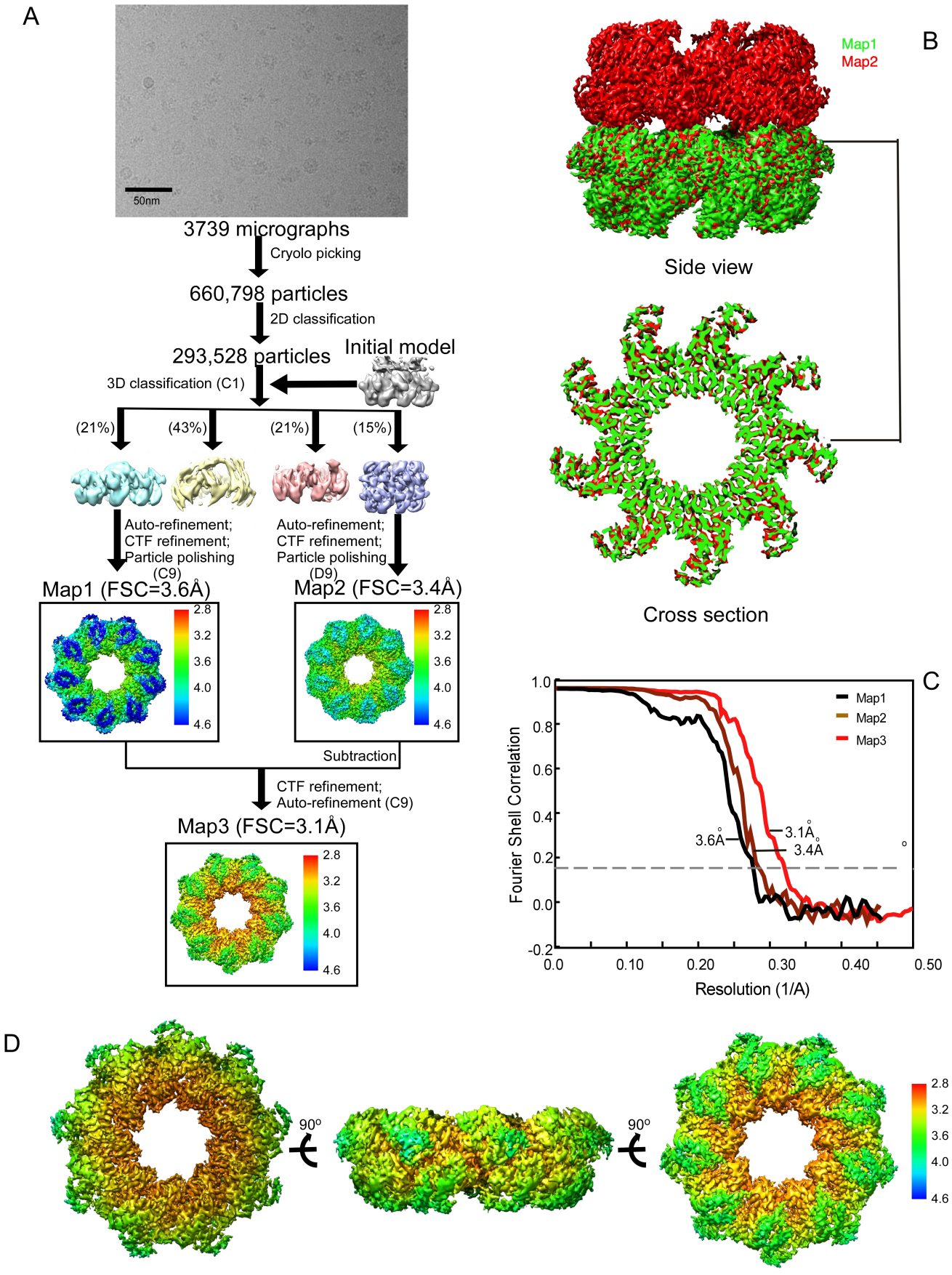

Fig. S7. Cryo-EM pipeline and structure analysis of SctV-C (related to Figure 4)

A. The cryo-EM data processing workflow.
B. Comparison of map1 and map2 reconstructed from single-ringed particles using C9 symmetry and from double ringed particles using D9 symmetry, separately. Cross-section of SctV-C shows that the map1 and map2 are well aligned.
C. Gold standard Fourier shell correlation (FSC) curves of the single-ringed map of SctV-C using single-ringed particles (black trace), double-ringed map of SctV-C using double-ringed particles (brown trace), and sing-ringed map of SctV-C using single-ringed particles and subtracted double-ringed particles (red trace).
D. Local resolution of the final cryo-EM map (map3) of SctV-C. The map was coloured according to local resolution with the indicated color key. The local resolution was calculated with Relion 3.1 and labeled in ChimeraX1.0.

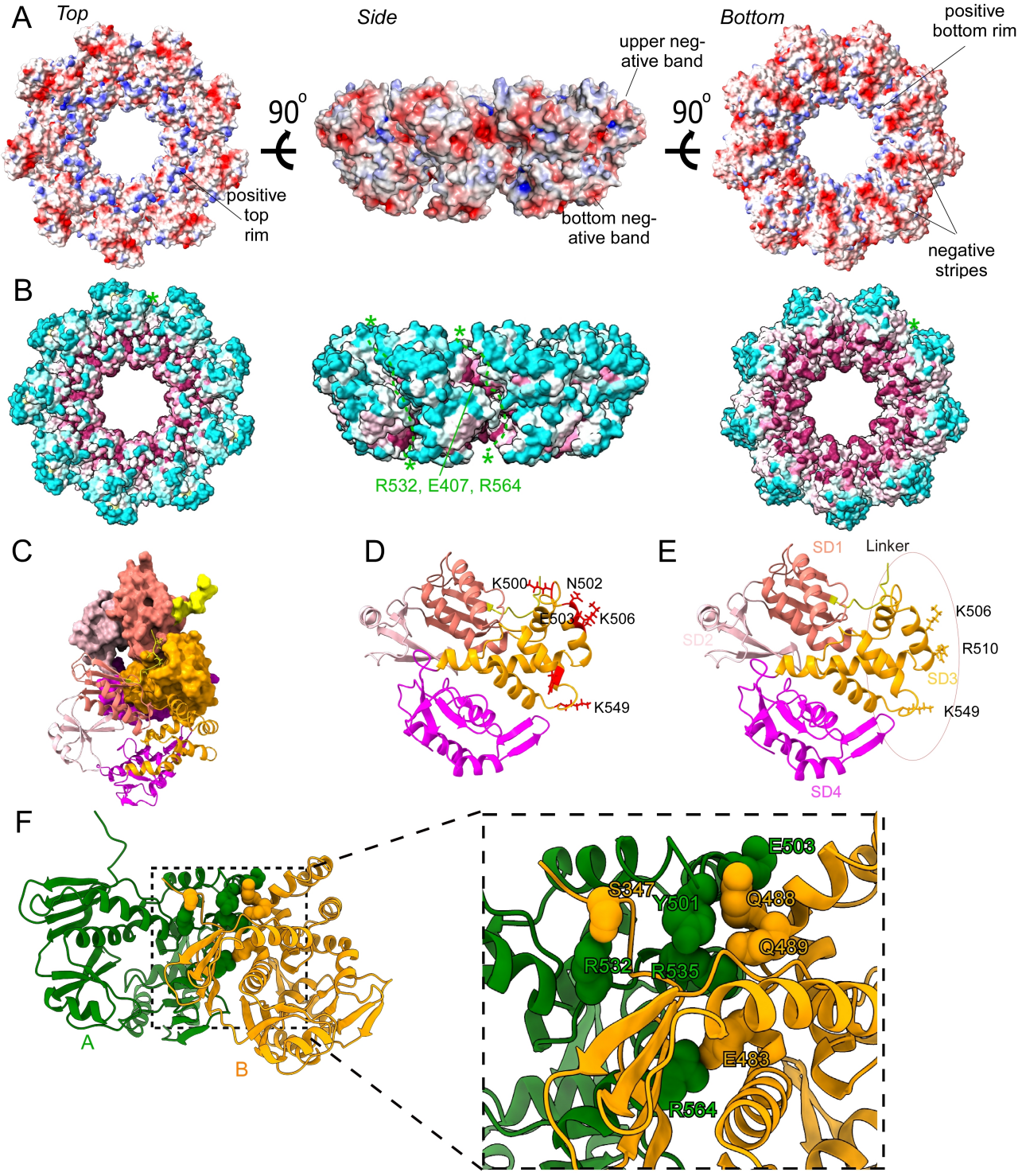

G

N-C linker-SD3 salt bridge	SD1-SD3 salt bridge	SD3-SD3 salt bridges	SD1-SD3 hinge
S347-R532(A)	E483-R564(A)	Q488(D)-E503(A)/Y501	484-487: FIG(T)V
		E489-R535(A)	

Fig. S8: Intraprotomeric domain organization/motions in the SctV-C protomer and close-up views of the interproteomeric interaction in the SctV-C nonamer (Related to Figures 2, 4, 6).

A. Electrostatic potential analysis of the SctV-C ring.The surface of the SctV-C ring was coloured by the electrostatic surface potential using ChimeraX. Possitive amino acids are Colored in blue, negative red and neutral white.

B. Sequence conservation analysis of the SctV-C ring. ConSurf (https://consurf.tau.ac.il/) was used to estimate the evolutionary conservation of SctV-C. The SctV-C ring is shown as a surface and is colored according to the ConSurf evolutionary conservation score (magenta very conserved to light blue no conservation). R532, E407 and R564 are shown with an asterisk in two adjacent protomers and a dashed line indicates the oligomerization interface.
C. Oligomerization interface of two adjacent protomers. The linker region of SctV-C protomer lying inside the small groove formed by SD1 and SD3 of its adjacent protomer. One protomer is shown as surface while the adjacent one in ribbon and both are colored as in Fig. 4B.
D. The side chains of the most mobile residues of SctV-C SD3 are shown and coloured in red
E. Ribbon diagram indicating the sub-domains of SctV-C (SD; SD1: 353-415 and 463-483; SD2:416-463; SD3: 488-570; SD4: 570-676). The protomer is shown in side view oriented as the orange protomer in 4A, side view**.** Conserved residues of SD3 that their side chains are protruding in the SctV pore are indicated.
F. The intermolecular electrostatic interactions that connect a protomer (A; green) to its neighbouring protomer (B; yellow) of $_{EPEC}$SctV-C shown here as spheres in the SctV-C model.
G. Mutagenesis analysis of the salt-bridges shown in D and of the flexible SD1-SD3 hinge (484-FIGV-487). The mutated residues are indicated in red. $_{EPEC}$SctV oligomerization mutants failed to restore protein secretion since they can not form oligomers, indicating that oligomerization is essential for T3SS (Fig. 2D-F; Fig. S6).

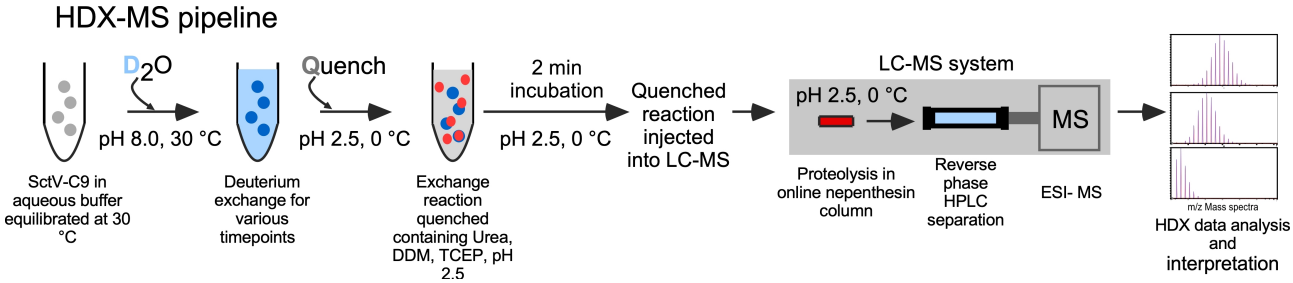

Fig. S9 HDX-MS pipeline and HDX-MS analysis of *EPEC*SctV-C (related to Figures 4 and 5).

Schematic representation of the HDX-MS pipeline for analyzing soluble EPECSctV-C. Soluble SctV-C_9 (5μM; grey circles) was diluted in deuterated buffer (1:10 dilution for 90% final D_2O concentration; 30°C; final volume 50μL) and incubated for different time points (10 s, 30 s, 1 m, 5 m, 10 m, 30 m, and 1440 m). The reactions were quenched with 50μL Buffer O, incubated for 2 min (4°C) and then injected into a LC-MS system (pH 2.5; 0°C; Waters) and digested using an on-line nepenthesin column (2.1 mm ID x 20 mm length, Cat. No.: AP-PC-004, Affipro) and peptides were separated using reverse phase HPLC C-18 analytical column (130 A°, 1.7 mm, 1 x 100 mm, Waters). HDX-MS data were analyzed and interpreted as described in experimental methods.

Supplementary Table:

Table S1. cryo-EM data and model refinement

SctV-C C9 map	
Data collection and processing	
Electron Microscope	Titan Krios
Electron Detector	K3 direct detector
Voltage (KV)	300
Pixel size	0.55
Electron exposure (e^-/ Å^2)	41.25
Defocus range(μm)	0-4
Symmetry imposed	C9
Number of micrographs	3739
Initial number of particles image	293,528
Final number of particles	105,670
Map resolution (Å)	3.1
FSC threshold	0.143
Map sharpening B factor (Å^2)	-94.52
Map resolution range (Å)	3.0-4.2
Initial model used	*Sf*SctV-C(4a5p)/*Sf*SctV-C(2x49)
Model composition	
Non-hydrogen atoms	
Protein residues	2935
Polypeptide chains	9
Bonds (Å)	0.010
Angles(°)	1.267
Ramachandran plot	
Favoured (%)	98.77
Allowed (%)	100
Outliers (%)	0
Validation	
MolProbity score	0.72
Clash score	0.67
Rotamer outlier (%)	0

Table S2. HDX-MS analysis data

Data Set	**SctV-C_9**
HDX reaction details	50 mM Tris, 50 mM KCl, pH_{read} = 8, 30 °C
HDX time course (min)	0.166, 0.5,1.0,5.0,10.0,30.0,100.0
HDX control samples	Maximally-labelled control (WT protein)
Back-exchange	20-45% (peptide composition dependent) Average=28%
# of Peptides	233
Sequence coverage	~99.7%
Average peptide length / Redundancy	8,70
Replicates (biological or technical)	2(biological), 3 x 3 (technical),
Repeatability (average standard deviation)	0,05
Significant differences in HDX (delta HDX > X D)	0.5 D (99.8% CI)

Table S3: SctV residues important for interactors to bind (related to Figures 6 and S6).

Mutated aa in SctV	Organism	Residue in $_{EPEC}$SctV	Ref.	Phenotype	
				Binding of interactors	Secretion
N373D	*S. flexneri*	Y362	(Shen and Blocker, 2016)	No interaction with SctW	middle substrates secretion: No late substrates secretion: Yes
I674V	*S. flexneri*	V658			
Q608R	*S. flexneri*	Q596			
Q626R	*P. aeruginosa*		(Lee et al., 2014)	No interaction with SctW domain 1 (Pcr1 protein)	late substrates secretion: Yes
G368C	*S. typhimurium* (Flagellum)	I354	(Inoue et al., 2019; Minamino and Namba, 2008)	Strong interaction with early substrates	Middle substrates secretion: No Late substrates secretion: No
D456V		S438	(Kinoshita et al., 2013)	Disturbs the binding site of chaperone-exported protein complexes	Reduced secretion and motility
F459A		S441			
T490M		F471			
I440A		F421	(Xing et al., 2018)	Disturbs the binding site of chaperone-exported protein complexes	Reduced motility
F459A		L437			
L461A		T439			
V482K		Y462			
V487G		D467			
D456A		D533			
^{427}DDLIE^{43}	*B. subtilis* (Flagellum)	^{428}ISFEF^{432}	(Bange et al., 2010)	Disturbs the binding site of chaperone-exported protein complexes	Reduced motility
^{445}KWISE^{44}		^{442}IVYKT^{446}			
^{453}DEADM^{4}		^{450}NQQLAHL^{456}			
F378V	*S. typhimurium*	F378	(Yu et al., 2018)	Disturbs the binding site of gatekeeper SctW	Middle substrates secretion: No Late substrates secretion: Yes (phenocopying secretion profile of gatekeeper deletion)
E488D		E489			
R531S		R532			
R509H		R510			
K515I		K516			
R590H		R591			
E591K/ L357F		E592/L357			
S592P		S593			
M450K/ I593N		N450/I593			
T596R		T597			
V632D		V632			

Supplementary materials:

Table S4. Buffers

Buffer A	50 mM Tris-HCl pH 8.0; 0.5 M NaCl; 5 mM Imidazole; 5% Glycerol
Buffer B	50 mM Tris-HCl pH 8.0; 50 mM NaCl; 5 mM Imidazole; 5% Glycerol
Buffer C	50 mM Tris-HCl pH 8.0; 50 mM NaCl; 150 mM Imidazole; 5% Glycerol
Buffer D	50 mM Tris-HCl pH 8.0; 50 mM NaCl; 10% Glycerol
Buffer E	50 mM Tris-HCl pH 8.0; 50 mM NaCl; 50% Glycerol
Buffer F	50 mM NaCl; 50 mM Tris-HCl(pH8.0); 2 mM 6-Aminohexanoic acid; 0.5 mM EDTA, 5 mM Imidazole; pH8.0
Buffer G	50 mM NaCl; 50 mM Tris-HCl pH8.0; 0.9% Triton X-100;5 mM Imidazole
Buffer H	50 mM NaCl; 50 mM Tris-HCl pH8.0; 5 mM Imidazole
Buffer I	50 mM Trizma base pH 8, 6.4 mM KCl, 170 mM NaCl
Buffer J	50 mM Trizma base pH 8, 50 mM KCl, 5mM $MgCl_2$, 5 g/L of sucrose, 100 µg/mL BSA, 0.01% v/v Tween-20
Buffer K	50 mM Trizma base pH 8, 2.7 mM KCl, 137 mM NaCl, 0.01% v/v Tween-20
Buffer L	1M NaCl; 50 mM Tris/HCl pH 8.0
Buffer M	50 mM NaCl; 50 mM Tris-HCl pH8.0
Buffer N	50mM Tris-HCl pH 8.0; 50mM KCl; 5mM $MgCl_2$
Buffer O	8MUrea; 5 mM TCEP; 0.1% DDM; Formic Acid 0.7%
1X PBS	137 mM $NaCl_2$; 2.7 mM KCl; 4.3 mM Na_2HPO_4; 1.4 mM KH_2PO_4
1XM9 salts	33.7 mM Na_2HPO_4; 22 mM KH_2PO_4; 8.55 mM NaCl; 9.35 mM NH_4Cl
Assembly Buffer	NSPr (an amphipathic bi-helical peptide) mix (1 fluorescent NSPr+ 2 non-fluorescent NSPr) in 20 mM Tris-HCl pH 8.0
Solubilization buffer	50 mM NaCl; 50 mM Tris-HCl pH7.0; 2 mM 6-Aminohexanoic acid; 1mM EDTA; 10% glycerol
BN-PAGE loading buffer	5% w/v Coomassie blue G-250 in 500mM 6-Aminohexanoic acid
Cathode buffer 1	50 mM Tricine pH 7.0; 7.5 mM Imidazole pH7.0; 0.02% w/v Coomassie blue G-250
Cathode buffer 2	50 mM Tricine pH 7.0; 7.5 mM Imidazole pH7.0; 0.002% w/v Coomassie blue G-250
Anode buffer	25 mM Imidazole pH 7.0

Table S5. Antisera

Rabbit polyclonal antibodies against the indicated purified proteins or protein domains were raised by Davids Biotechnologie, Germany. Antibodies against T3SS-related proteins were further purified by 9 cycles of negative immuno-absorption, using membranes isolated from EPEC strains that lacked the gene of interest, i.e. for α-SctJ, membranes isolated from EPEC Δ*sctJ* cells were used.

Antibody	Animal Source	Reference or commercial source
α-SctV-C	Rabbit	(Portaliou et al., 2017)
α-SctU-C	Rabbit	This study
α-GFP	Rabbit	(Hamed et al., 2018)
α-CesT	Rabbit	(Portaliou et al., 2017)
α-CesF	Rabbit	(Portaliou et al., 2017)
α-Rabbit IgG	Goat	Jackson ImmunoResearch Europe Ltd
α-His tag	Mouse	SEROTEC
α-Mouse IgG	Goat	Jackson ImmunoResearch Europe Ltd

Table S6. Bacterial strains

Bacterial strain *E. coli*	**Description (gene deleted)**	**Reference/source**
DH5a	F⁻ *endA1 glnV44 thi-1 recA1 relA1 gyrA96 deoR nupG purB20* φ80d*lacZ*ΔM15 Δ(*lacZYA-argF*)U169, hsdR17($r_K^- m_K^+$), λ⁻	Invitrogen
BL21(DE3)	*E. coli* str. B F⁻ *ompT gal dcm lon hsdS*$_B$($r_B^- m_B^-$) λ(DE3 [*lacI lacUV5-T7p07 ind1 sam7 nin5*]) [*malB*$^+$]$_{K\text{-}12}$(λ^S)	(Studier et al., 1990)
C41(DE3)	F⁻ *ompT gal dcm hsdS*$_B$($r_B^- m_B^-$)(DE3)	Lucigen (Miroux and Walker, 1996)
EPEC E2348/69	*E. coli* O127:H6 (strain E2348/69)	(Levine et al., 1978)
EPEC E2348/69 Δ*sctV*	Δ*sctV*:: *nptII*(Kan^R)	(Portaliou et al., 2017)

Table S7. Vectors and genetic constructs:
Genes were cloned in the indicated plasmid vectors using a combination of restriction sites (as indicated). DNA restriction enzymes and DNA polymerases were from Promega. All PCR-generated plasmids were sequenced (Macrogen, Europe). Plasmids were transformed in DH5α cells and stored in 20% glycerol at –80ºC.

Vector name	**Antibiotic resistance**	**Promoter**	**Origin**	**Reference/source**
pASKIBA7	Amp	Tet	pBR322	IBA life sciences; (Guzman et al., 1995)
pETDuet-1	Amp	T7	pBR322	Novagen
pACYCDuet-1	Cm	T7	p15A	Novagen
pET16b	Amp	T7	pBR322	Novagen
pBAD501	Gm	pBAD	p15A	(Chatzi et al., 2017)
pBAD24	Amp	pBAD	pBR322	(Guzman et al., 1995)
Gene	**Uniprot KB accession**	**Plasmid name**	**Vector**	**Cloning strategy or source**
sctV	B7UMA7	pLMB1823	pACYCDuet-1	The *sctV* gene was digested out from pETDuet1-*sctV* (pLMB0057) and inserted in pACYCDuet1 after NdeI-XhoI digestion.
sctV	B7UMA7	pLMB0088	pASKIBA 7	(Portaliou et al., 2017)
sctV $\gamma-$	B7UMA7	pLMB1764	pASKIBA 7	(Portaliou et al., 2017)
sctV $\varepsilon-$	B7UMA7	pLMB1765	pASKIBA 7	The synthetic gene fragment of *sctV* (sgLMB017) was digested out and inserted to pASK sctV- no HindIII (pLMB1912).
his-sctV	B7UMA7	pLMB1840	pACYCDuet-1	The *sctV* gene was amplified from EPEC E2348/69 (B1030) using primers X2126 and X1710. The gene was inserted at the 2nd multiple cloning site of pACYCDuet-1 after NdeI and XhoI digestion.
his-sctV	B7UMA7	pLMB1877	pASKIBA500	The *his-sctV* gene was digested out from pLMB1840 (pACYCDuet1-*his-sctV*) using NdeI-XhoI restriction enzymes and inserted in pASK500 at the same sites.
his-sctV	B7UMA7	pLMB1841	pBAD501	The *his-sctV* gene was digested out from pLMB1840 (pACYCDuet1-*his-sctV*) using NdeI-XhoI restriction enzymes and inserted in pBAD501 at the same sites.
his-sctRSTU	B7UMB8 B7UMB9 B7UMC0 B7UMC1	pLMB1824	pET Duet 1	The *sctR/S/T/U* genes were amplified from EPEC E2348/69 (B1030) using primers X1725 and X1527. The genes were inserted

				at the 2nd multiple cloning site of pet Duet-1 after NcoI and BamHI digestion.
his-sctV(N1-333)	B7UMA7	pLMB1881	pET16b	The *sctV* (N1-333) fragment was amplified from EPEC E2348/69 (B1030) using primers X1709 and X2132. The gene was inserted in pET16b after NdeI and XhoI digestion.
his-sctVc(N334-675)	B7UMA7	pLMB1676	pET16b	(Portaliou et al., 2017)
*his-sctVc (*E503A)	B7UMA7	pLMB2140	pET16b	pLMB1676 was used to generate the *his-sctVc(*E503A*)* mutant by site directed mutagenesis
*his-sctVc (*R532A)	B7UMA7	pLMB2141	pET16b	pLMB1676 was used to generate the *his-sctVc(*R532A*)* mutant by site directed mutagenesis
*his-sctVc (*R535*A)*	B7UMA7	pLMB2142	pET16b	pLMB1676 was used to generate the *his-sctVc(*R535A*)* mutant by site directed mutagenesis
*his-sctVc (*R564A*)*	B7UMA7	pLMB2143	pET16b	pLMB1676 was used to generate the *his-sctVc(R564A)* mutant by site directed mutagenesis
*his-sctVc (*E503A/R535A*)*	B7UMA7	pLMB2144	pET16b	pLMB2140 was used to generate the *his-sctVc(*E503A/R535A) mutant by site directed mutagenesis
*his-sctVc (*E503A/R535A/ R564A*)*	B7UMA7	pLMB2145	pET16b	pLMB2144 was used to generate the *his-sctVc(*E503AR/535AR/564A) mutant by site directed mutagenesis
*his-sctVc (*G486T)	B7UMA7	pLMB2137	pET16b	pLMB1676 was used to generate the *his-sctVc(*G486T*)* mutant by site directed mutagenesis
*his-sctVc (*Q488D*)*	B7UMA7	pLMB2138	pET16b	pLMB1676 was used to generate the *his-sctVc(*Q488D*)* mutant by site directed mutagenesis
*his-sctVc (*G486T/Q488D*)*	B7UMA7	pLMB2139	pET16b	pLMB2137 was used to generate the *his-sctVc(*G486T/Q488D*)* mutant by site directed mutagenesis
*sctV(*E503A*)*	B7UMA7	pLMB2131	pASKIBA7	pLMB0088 was used to generate the *his-sctV(*E503A*)* mutant by site directed mutagenesis
*sctV(*R532A*)*	B7UMA7	pLMB2132	pASKIBA7	pLMB0088 was used to generate the *his-sctV(*R532A*)* mutant by site directed mutagenesis
sctV(R535A*)*	B7UMA7	pLMB2133	pASKIBA7	pLMB0088 was used to generate the *his-sctV(*R535A) mutant by site directed mutagenesis
*sctV(*R564A*)*	B7UMA7	pLMB2134	pASKIBA7	pLMB0088 was used to generate the *his-sctV(*R564A) mutant by site directed mutagenesis
*sctV(*E503A/R535A)	B7UMA7	pLMB2135	pASKIBA7	pLMB2131 was used to generate the *his-sctV(*E503A/R535A*)* mutant by site directed mutagenesis
*sctV(*E503A/R535AR/564A*)*	B7UMA7	pLMB2136	pASKIBA7	pLMB2135 was used to generate the *his-sctV(*E503A/R535A/R564A*)* mutant by site directed mutagenesis
*sctV(*G486T*)*	B7UMA7	pLMB2128	pASKIBA7	pLMB0088 was used to generate the *his-sctV(*G486T*)* mutant by site directed mutagenesis
*sctV(*Q488D)	B7UMA7	pLMB2129	pASKIBA7	pLMB0088 was used to generate the *his-sctV(*Q488D*)* mutant by site directed mutagenesis

*sctV(*G486T/Q488D)	B7UMA7	pLMB2130	pASKIBA7	pLMB0088 was used to generate the *his-sctV(*G486T/Q488D*)* mutant by site directed mutagenesis
eyfp-sctV	B7UMA7	pLMB1800	pASK IBA500-*eyfp*-MCS	The *sctV* gene was digested out from pLMB0088 (pASKIBA7-*sctV*) and was inserted in pLMB1774 (pASK500-*eyfp*-MCS) after NheI-XhoI digestion.
torA-gfp	---	---	pBAD24	(Barrett et al., 2003)
lacY-eyfp	---	---	pBAD/His	(Robinson et al., 2015)
eyfp	---	pLMB1774	pASKIBA500	The 800bp *eyfp* gene was amplified from pLMB1707 using primers X2058 and X2062. The gene was inserted in pASKIBA500 (pLMB0014) after XbaI-NdeI digestion.
his-cesT	P21244	pIMBB1157	pETDuet-1	(Portaliou et al., 2017)
his-cesT and tir	P21244 and B7UM99	pIMBB1158	pETDuet-1	(Portaliou et al., 2017)
bamE-gfp	P0A937	pDR*bamE*-GFP	pDRGFP	R. Ieva
his-cesF	B7UM99	pIMBB664	pETDuet-1	(Portaliou et al., 2017)
his-espF	B7UM88	pIMBB612	pET22b	The *espF-his* gene was amplified from EPEC E2348/69 (B1030) using primers X342 and X344 and inserted in pET22b vector after NdeI- XhoI digestion.

Table S8. List of primers used for gene cloning

Primer Name	Gene	Restriction site	Forward/ Reverse	Sequence (5'-3') (restriction sites underlined/ linker italics/ mutation bold)
X2126	his-*sctV*	*NdeI*	Forward	GGAATTCCATATGCATCACCATCATCACCACATGAATAA ACTCTTAAATATATTTAAAA
X1710	*his-sctV*	*XhoI*	Reverse	GGCCTCGAGTCATGCTCTGAAATCATTTAC
X1709	*his-sctV*(N1-333)	*NdeI*	Forward	GGAATTCCATATGAATAAACTCTTAAATATATTTAAAA
X2132	*his-sctV*(N1-333)	*XhoI*	Reverse	GACCCGCTCGAGTTACTTATTATTGCCAGCTCCAAAT
X342	*espF*	*NdeI*	Forward	GGGAATTCCATATGCTTAATGGAATTAGTAACGCTG
X344	*espF*	*XhoI*	Reverse	CCGCTCGAGCCCTTTCTTCGATTGCTCATAGGC
X2058	*eyfp*	*XbaI*	Forward	GCGGTCTAGATAACGAGGGCAAAAAATGGGTAGCATGGT
X2062	*eyfp*	*NdeI*	Reverse	GGGAATTCCATATG*AGAGCCTCCGCCAGAGCCTCCGCC*C TTGTACAGCTCGTCCATGCCGAG
X1725	*his-sctRSTU*	*NcoI*	Forward	CATGCCATGGGCAGCAGCCATCACCATCATCACCACATG TCTCAATTAATGACCATTGG
X1527	*his-sctRSTU*	*BamHI*	Reverse	CGCGGATCCTTAATAATCAAGGTCTATCGCAATAC
-	*sctVE503A*		Forward	GAGAGAAAATATAAC**GCT**CTTGTGAAAGAGCTG
-	*sctVE503A*		Reverse	CAGCTCTTTCACAAG**AGC**GTTATATTTTCTCTC
-	*sctVR532A*		Forward	GAAAATGTCTCAATT**GCA**GATCTGAGAACTATC
-	*sctVR532A*		Reverse	GATAGTTCTCAGATC**TGC**AATTGAGACATTTTC
-	*sctVR535A*		Forward	TCAATTAGAGATCTG**GCA**ACTATCTTTGAGACG
-	*sctVR535A*		Reverse	TCAATTAGAGATCTG**GCA**ACTATCTTTGAGACG
-	*sctVR564A*		Forward	CGTATCGCCCTGCGT**GCT**CATATTTTAGGTCGC
-	*sctVR564A*		Reverse	GCGACCTAAAATATG**AGC**ACGCAGGGCGATACG
-	*sctVG486T*		Forward	GCCAAAGAGTTCATC**ACT**GTACAAGAAACGCGT
-	*sctVG486T*		Reverse	ACGCGTTTCTTGTAC**AGT**GATGAACTCTTTGGC
-	*sctVQ488D*		Forward	GAGTTCATCGGCGTA**GAT**GAAACGCGTTATTTG
-	*sctVQ488D*		Reverse	CAAATAACGCGTTTC**ATC**TACGCCGATGAACTC
-	*sctVG486TQ488D*		Forward	GAGTTCATCACTGTA**GAT**GAAACGCGTTATTTG

-	*sctVG486TQ488D*		Reverse	CAAATAACGCGTTTC**ATC**TACAGTGATGAACTC

Supplementary movies:

Movie S1: Sub-domain motions of SctV-C

$_{EPEC}$SctV-C was compared to the virulence T3SS homologues $_{Cp}$SctV-C from *Chlamydia pneumoniae* (Jensen et al., 2020)(PDB:6WA6) represennting the "open" state and $_{Sf}$SctV-C(PDB: 2x49) from *Salmonella typhimurium* (Worrall et al., 2010) representing the "closed" state. The structure of $_{EPEC}$SctV-C resolved here by cryo-EM (Fig. 4A) was classified as a "intermediate" state.

Movie S2: Highly dynamic regions obtained from HDX-MS analysis.

Only the highly flexible regions derived from the HDX-MS analysis are included (Fig. S6E, red)

Movie S3: Chaperone binding sites mapped on one protomer of SctV$_9$

Binding sites are from NMR data (Xing et al., 2018) and patches α,β and γ from pepscan analysis [Fig. S6E; (Portaliou et al., 2017)].

Movie S4: Binding sites of the ATPase inner stalk protein SctO mapped on two adjacent protomers of SctV$_9$

Supplementary methods:

Preparation of cells for live-cell fluorescence microscopy

Bacterial strains were transformed with indicated plasmids and grown overnight at 37ºC on LB agar plates supplemented with the appropriate antibiotics. An overnight pre-culture starting from one single colony from the LB plates was inoculated in EZ rich defined medium (1:100 dilution; Teknova) with 0.2% w/v glucose as the carbon source and specific antibiotics until OD_{600} reached 0.3-0.4. Gene expression was induced with AHT (as indicated) at 37ºC for 30-60 min. Cells were pelleted by centrifugation at 3,000 x g for 3 min to remove the inducer and resuspended in fresh EZ rich medium before imaging. Coverslips were firstly cleaned by sonicating in 5M KOH for 1h, and then rinsed with deionized water several times and dried with nitrogen. Following the cleaning step, coverslips were treated by Oxygen plasma cleaning for 10 min (PE-50 Compact Bench-top Plasma Cleaning System, Plasma Etch) to remove contaminants from the glass surfaces. Cells were sandwiched between a clean glass cover slip and an agarose slab (10 mg/mL Agarose; low gelling temperature; Sigma-Aldrich) and imaged with live-cell fluorescence microscopy.

Western blotting analysis

Following SDS-PAGE or Native-PAGE analysis, proteins were transferred onto nitrocellulose membrane (PROTRAN) or PVDF membrane (Thermo Scientific) using Semi-Dry Transfer apparatus (BIORAD) following manufacturer's instruction (20V; 20 min for SDS-PAGE; 40 min for Native-PAGE). After antibody staining, membranes were incubated with SuperSignal™ West Pico PLUS chemiluminescent substrate (Thermo Scientific) for 2 min for signal development. Images were acquired using Las4000 (GE Healthcare). For image acquisition the manufacturer's setting were used (Resolution / Sensitivity: standard mode; Exposure time 10-20 min; Image dimensions 210 x 140 mm; Image resolution 176 dpi).

Sub-cellular protein localization of SctV cytoplasmic or transmembrane domain

C41 cells carrying either pETDuet-*sctV,* or His-*sctV*N1-333 or His *sctV*-C were induced with 0.2 mM IPTG for 12 hours, at 18ºC. Bacteria were resuspended in Buffer A and lysed with French press. Unbroken cells were removed (3,000 x g; 10 min; 4ºC) before high-speed centrifugation (100,000 x g; 30 min; 4 ºC;45 Ti rotor; Optima XPN-80; Beckman Coulter). Sequential washes with 8M urea overnight and 2 hours at room temperature were introduced, when indicated, to remove the inclusion bodies of expressed proteins associated with the membrane. Equal amounts of cytosolic or membrane proteins were analyzed on 12% acrylamide gels by SDS-PAGE and immuno-stained.

Peptide array analysis

Peptide array analysis was performed as described previously (Karamanou et al., 2008; Portaliou et al., 2017). In brief, 13mer-, overlapping peptides of SctV-C were immobilized on cellulose membranes (PepSpot Peptides; JPT Peptide Technologies; Germany). Before screening, the dry membrane was washed in methanol (10 min), in high-salt buffer I at room temperature (3 × 5 min), in buffer I at the desired temperature (5 × 5 min) and finally in equilibration buffer J (15 min). 200 nM of chaperones or the chaperone/exported protein complexes were incubated with the peptide array membrane for 30 min at 25°C. Unbound complexes were removed with extended washes with buffer K. The proteins bound to peptides were electro-transferred onto PVDF membrane (Thermo Scientific). Bound proteins to specific peptides were visualized by western-blot using specific antibodies.

Determination of equilibrium dissociation constants (K_d)

Equilibrium dissociation constants determination was conducted as described previously (Gouridis et al., 2009; Portaliou et al., 2017). In brief, the [35^S]-labelled proteins were labelled *in vitro* using the Easy TagTM L-[35^S]-methionine (1 mC, Perkin Elmer) and the TNT® Quick coupled Transcription/Translation systems (Promega), according to the manufacturer's instructions.

Proteins and protein complexes stored in Buffer E were serially diluted in Buffer N (20 concentration points; 0.01-1 μM) and mixed with IMVs (20 μg total membrane protein/reaction; 20 μl in Buffer N). 1μl of [^{35}S]-labelled protein was added to all the reactions, as a tracer. Samples were incubated on ice for 20 min, and then overlaid on an equal volume of BSA/sucrose cushion (0.2 M Sucrose; 1 mg/mL BSA in Buffer N) and centrifuged (300,000 x g; 20 min; 4°C; rotor TLA-100; Optima Max-XP, Beckman-Coulter). The pellet (containing IMVs and IMVs-bound proteins) was resuspended in 300 μl Buffer N by using a water-bath sonicator and proteins were immobilized on a nitrocellulose membrane using a vacuum manifold (Bio-Dot apparatus; Bio-Rad). Binding of [35^S]-labelled proteins on IMVs was visualized by using a high-resolution phosphor storage screen (GE Healthcare) on a Typhoon FLA 9500 system (GE Healthcare; default settings). Image Quant software (GE Healthcare) was used for signal quantification. Data were analyzed by non-linear regression fit for one binding site, using Prism 6.0 (GraphPad). For the determination of each K_d, $n=6$, each using 20 concentration points.

Native mass spectrometry

His-SctV-C9 was dialyzed in 50 mM ammonium acetate and analyzed using electrospray ionization mass spectrometer (ESI-MS) with a Q-TOF mass analyzer (Synapt G2 HDMS, Waters) and sodium iodide (2 mg/mL) as a calibrant. The operating parameters for the spectral acquisition were as follows: capillary voltage, 1.8 kV; sample cone voltage, 60 V; extraction cone voltage, 2 V; source temperature, 80°C; desolvation temperature, 150°C; backing pressure, 5.26 mbar; source pressure, 2.08 e-3 mbar; Trap, 1.44 e-3 mbar. Spectra were acquired in the range of 900–8000 m/z in positive-ion V mode. The molecular mass of the recorded spectra was calculated using MassLynx software (MassLynx version 4.1) by deconvoluting the mass spectra using MaxEnt 1.

References

Bange, G., Kümmerer, N., Engel, C., Bozkurt, G., Wild, K., and Sinning, I. (2010). FlhA provides the adaptor for coordinated delivery of late flagella building blocks to the type III secretion system. Proceedings of the National Academy of Sciences *107*, 11295-11300.
Barrett, C.M., Ray, N., Thomas, J.D., Robinson, C., and Bolhuis, A. (2003). Quantitative export of a reporter protein, GFP, by the twin-arginine translocation pathway in Escherichia coli. Biochemical and biophysical research communications *304*, 279-284.
Chatzi, K.E., Sardis, M.F., Tsirigotaki, A., Koukaki, M., Sostaric, N., Konijnenberg, A., Sobott, F., Kalodimos, C.G., Karamanou, S., and Economou, A. (2017). Preprotein mature domains contain translocase targeting signals that are essential for secretion. The Journal of cell biology *216*, 1357-1369.
Guzman, L.M., Belin, D., Carson, M.J., and Beckwith, J. (1995). Tight regulation, modulation, and high-level expression by vectors containing the arabinose PBAD promoter. J Bacteriol *177*, 4121-4130.
Hamed, M.B., Vrancken, K., Bilyk, B., Koepff, J., Novakova, R., Van Mellaert, L., Oldiges, M., Luzhetskyy, A., Kormanec, J., and Anné, J.J.F.i.m. (2018). Monitoring protein secretion in Streptomyces using fluorescent proteins. *9*, 3019.
Inoue, Y., Ogawa, Y., Kinoshita, M., Terahara, N., Shimada, M., Kodera, N., Ando, T., Namba, K., Kitao, A., Imada, K*., et al.* (2019). Structural Insights into the Substrate Specificity Switch Mechanism of the Type III Protein Export Apparatus. Structure *27*, 965-976 e966.
Jensen, J.L., Yamini, S., Rietsch, A., and Spiller, B.W. (2020). "The structure of the Type III secretion system export gate with CdsO, an ATPase lever arm". PLoS pathogens *16*, e1008923.
Karamanou, S., Bariami, V., Papanikou, E., Kalodimos, C.G., and Economou, A.J.M.m. (2008). Assembly of the translocase motor onto the preprotein-conducting channel. *70*, 311-322.
Kinoshita, M., Hara, N., Imada, K., Namba, K., and Minamino, T.J.M.m. (2013). Interactions of bacterial flagellar chaperone–substrate complexes with FlhA contribute to co-ordinating assembly of the flagellar filament. *90*, 1249-1261.
Lee, P.-C., Zmina, S.E., Stopford, C.M., Toska, J., and Rietsch, A.J.P.o.t.N.A.o.S. (2014). Control of type III secretion activity and substrate specificity by the cytoplasmic regulator PcrG. *111*, E2027-E2036.
Levine, M.M., Bergquist, E.J., Nalin, D.R., Waterman, D.H., Hornick, R.B., Young, C.R., and Sotman, S. (1978). Escherichia coli strains that cause diarrhoea but do not produce heat-labile or heat-stable enterotoxins and are non-invasive. Lancet *1*, 1119-1122.
Minamino, T., and Namba, K.J.N. (2008). Distinct roles of the FliI ATPase and proton motive force in bacterial flagellar protein export. *451*, 485.
Miroux, B., and Walker, J.E.J.J.o.m.b. (1996). Over-production of proteins in Escherichia coli: mutant hosts that allow synthesis of some membrane proteins and globular proteins at high levels. *260*, 289-298.
Portaliou, A.G., Tsolis, K.C., Loos, M.S., Balabanidou, V., Rayo, J., Tsirigotaki, A., Crepin, V.F., Frankel, G., Kalodimos, C.G., and Karamanou, S. (2017). Hierarchical protein targeting and secretion is controlled by an affinity switch in the type III secretion system of enteropathogenic Escherichia coli. The EMBO journal *36*, 3517-3531.
Robinson, A., McDonald, J.P., Caldas, V.E., Patel, M., Wood, E.A., Punter, C.M., Ghodke, H., Cox, M.M., Woodgate, R., and Goodman, M.F.J.P.g. (2015). Regulation of mutagenic DNA polymerase V activation in space and time. *11*, e1005482.
Shen, D.-K., and Blocker, A.J.J.P.o. (2016). MxiA, MxiC and IpaD regulate substrate selection and secretion mode in the T3SS of Shigella flexneri. *11*, e0155141.

Smit J.H., K.S., Srinivasu B.,Y., Karamanou S., Economou A. (2020). PyHDX: Derivation and visualization of protection factors from Hydrogen-Deuterium Exchange Mass Spectrometry at near residue resolution. bioRxiV.
Studier, F.W., Rosenberg, A.H., Dunn, J.J., and Dubendorff, J.W. (1990). Use of T7 RNA polymerase to direct expression of cloned genes. Methods Enzymol *185*, 60-89.
Worrall, L.J., Vuckovic, M., and Strynadka, N.C. (2010). Crystal structure of the C-terminal domain of the Salmonella type III secretion system export apparatus protein InvA. Protein science : a publication of the Protein Society *19*, 1091-1096.
Xing, Q., Shi, K., Portaliou, A., Rossi, P., Economou, A., and Kalodimos, C.G. (2018). Structures of chaperone-substrate complexes docked onto the export gate in a type III secretion system. Nature communications *9*, 1773.
Yu, X.-J., Grabe, G.J., Liu, M., Mota, L.J., and Holden, D.W.J.m. (2018). SsaV interacts with SsaL to control the translocon-to-effector switch in the Salmonella SPI-2 type three secretion system. *9*, e01149-01118.